International Journal of Wireless Communications and Mobile Computing
2015; 3(2): 13-17
Published online February 25, 2015 (http://www.sciencepublishinggroup.com/j/wcmc)
doi: 10.11648/j.wcmc.20150302.11
ISSN: 2330-1007 (Print); ISSN: 2330-1015 (Online)

Array Antennas Comprised of Tetragons for RFID Applications

Manato Fujimoto, Yukio Iida*

Department of Electrical and Electronic Engineering, Faculty of Engineering Science, Kansai University, Osaka, Japan

Email address:
manato@jnet.densi.kansai-u.ac.jp (M. Fujimoto), iida@kansai-u.ac.jp (Y. Iida)

To cite this article:
Manato Fujimoto, Yukio Iida. Array Antennas Comprised of Tetragons for RFID Applications. *International Journal of Wireless Communications and Mobile Computing*. Vol. 3, No. 2, 2015, pp. 13-17. doi: 10.11648/j.wcmc.20150302.11

Abstract: The location estimation capability of a RFID (Radio Frequency Identification) technology is useful for indoor navigation systems on mobile robots. In this paper, we study a simple and small structural antenna at 2.5GHz band that can reduce the beam when installed on a mobile robot. An antenna with small occupation volume by a mechanical rotation is assumed. We used electromagnetic field simulation and experimental results to design a simple structural antenna. Our design culminates in two antennas comprised of Tetragon elements formed with wires. One is called Tetra-4, and is an antenna which has a lateral arrangement of four tetragons. Because the input impedance is considerably high, Tetra-4 is suitable for use in the high impedance system. When driving in 100 Ω balanced system, the gain of Tetra-4 is 8dBi. The half-power band width (HPBW) in the H-plane is 38 degrees, and is 0.44 times that of a dipole with a reflector. Another one is Yagi-Uda antenna comprised of two tetragon elements. When driving in 50 Ω balanced system, the gain is 11dBi. The HPBW is 40 degrees in the H-plane and is 36 degrees in the E-plane.

Keywords: Array Antenna, Tetragon, Loop Antenna, RFID, Location Estimation, Mobile Robot

1. Introduction

Recently, RFID (Radio Frequency Identification) technology has attracted attention around the world as a new approach to achieving ubiquitous environments [1]. RFID technology is used in various fields due to features such as having a simple composition, being inexpensive, making it very easy to store information in the memory of a RFID tag, etc. In particular, the estimation of the location of RFID tags has attracted attention from many researchers [2]-[7]. If the location estimation of RFID tags is achieved, it can be used in various applications (for example, indoor navigation systems on mobile robots, etc.) [8]-[11].

A large antennas are used though the experiment with the robot and the wheelchair is conducted [12], [13]. Because the robot is not only work of self-positional recognition, a small antenna is preferable. We also have done a lot of experiments and the simulations [5]-[7], [11], [14]. As a result, we feel the necessity of the antenna that doesn't disturb the movement of the robot strong. The antenna for the robot will be needed more and more in the future. Then, a simple and small antenna that can reduce the beam width for use in mobile robots is studied in this paper. The antenna with small occupation volume by a mechanical rotation is assumed.

We consider a passive tag that is supplied with power from the electromagnetic waves of a reader/writer. A passive tag requires a strong electromagnetic field above a certain level in order to obtain sufficient power. Therefore, for the array antenna considered here, the radiation range of the peak level is very important, unlike antennas using for normal communications.

When the direction in a horizontal plane is detected by arranging tag for a linearly polarized wave, the radiation pattern in a horizontal plane is important. The antenna with narrow beam width is necessary in a horizontal plane. When it is necessary to detect the vertical position, the antenna with narrow beam width is necessary also for the vertical direction.

In recent years, the electromagnetic wave applications has increased. Various antennas have attracted attention due to their simplicity, cost effectiveness, and ease of manufacturing, etc. [15]-[17]. In addition, there are many studies in relation to loop antennas [18]-[23]. These reports are mostly based on the basic loop antenna and Yagi-Uda antenna. In this paper, we will study an array antenna based on a tetragonal structure.

This paper is organized as follows. Section 2 explains basic antenna structures of Tetra-1, Tetra-2, and Tetra-4 using this paper. Section 3 presents basic characteristics of each antenna through electromagnetic field simulations using FDTD method. Section 4 shows experimental results of Tetra-4 antenna. Section 5 presents the Yagi-Uda antenna comprised of two tetragon elements. Finally, we conclude this paper in Section 6.

2. Basic Structure of Antennas

In this section, we will investigate the round loop antenna and radiation principle. The necessary current for electromagnetic radiation flows when the circumference is equal to one wavelength. Since the direction of the current reverses for each half wavelength, an electromagnetic wave of a linear polarization is radiated. We designed a suitable structure using the radiation principle, and performed electromagnetic field simulations and corresponding experimental analysis. In this study, we are primarily interested in the development of an antenna that uses a wire to form a narrowly focused beam. We groped the resonating structures based on their suitability for the radiation of electromagnetic wave. As one of results, we arrived at the tetragonal structure shown in Figure 1.

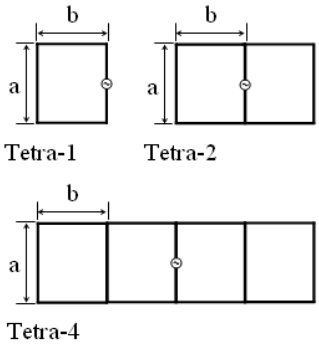

Figure 1. *The basic structure of each antenna.*

Figure 1 shows the basic structure of the antenna studied in this paper. Each antenna, Tetra-1, Tetra-2, and Tetra-4, is labeled according to the number of tetragons. In this paper, it is assumed that the antenna is used in the vicinity of 2.5 GHz (wavelength λ = 120 mm). Since the loop antenna resonates when the wavelength is equal to a round of the loop, the tetragon was formed such that the length of one loop is 120 mm. We set a =32mm and b = 28mm. The antennas were produced using copper wire of 2.0 mm in diameter.

3. Basic Characteristics through Electromagnetic Field Simulations

3.1. Simulation Method of the Electromagnetic Field

In this section, we investigate the basic characteristics of the antenna through electromagnetic field simulations using the FDTD (Finite-Difference Time-Domain) method. The structure of the antenna was discretized into 2 mm square cubes. Since the structure of each antenna is discretized into 2 mm blocks, the size of the antenna in these simulations is a = 32 mm and b = 28 mm for the tetragons.

Figure 2 shows the Tetra-4 antenna and the simulation region. We placed the electric wall at the YZ-plane at X = 0 and analyzed the space of the upper half. The FDTD cell size was $\Delta x = \Delta y = \Delta z = 2$ mm. In order to simplify the representation, we used $X = x/\Delta x$, $Y = y/\Delta y$, and $Z = z/\Delta z$ as normalized coordinates.

In Section 2, we used the antennas shown in Figure 1. We assume that each antenna studied in this paper is attached to a mobile robot. From this assumption, the conductor plane should be placed at the back of the antenna. In Figure 2, the conductor board is placed at Z = 0 and the antenna surface is placed at Z = 30 (= λ/4).

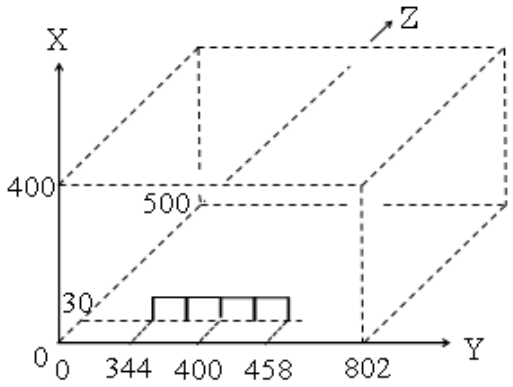

Figure 2. *Tetra-4 antenna and analysis region.*

3.2. Radiation Intensity and Beam Width

In the analysis area defined, we examined the electromagnetic field distribution on the line Y = 100 ~ 700 at Z = 360. The results are summarized in Figure 3. The vertical axis is given as P_r/P_{in}. Here, P_{in} is the active power that enters the antenna. P_r represents the electric field strength converted into the received power of the isotropic antenna and is the power that can be received when the isotropic antenna is placed at the observation line at Z = 360. We call P_r/P_{in} the radiation intensity. The gain of Hexa-4 is 3.4 dB higher than that of a dipole. The dipole here is an antenna with a reflector (conductor board).

The radiation intensity shows the performance of the antenna without any relation to the input impedance. The input impedance of the antenna is particularly important for achieving a suitable connection to the power feeding system. As for the power feeding system of the antenna, an unbalanced system at 50 Ω and 75 Ω is often used. The performance evaluation of an antenna that is independent of specific impedance is important if the antenna is required to operate with a variety of feed systems.

We considered the 3dB range of the Y coordinate which decreased by 3 dB from the maximum radiation intensity. The 3 dB range narrowed as the tetragon increased. The 3 dB range was 309 with Tetra-4, and was 66% of the 468 of a dipole.

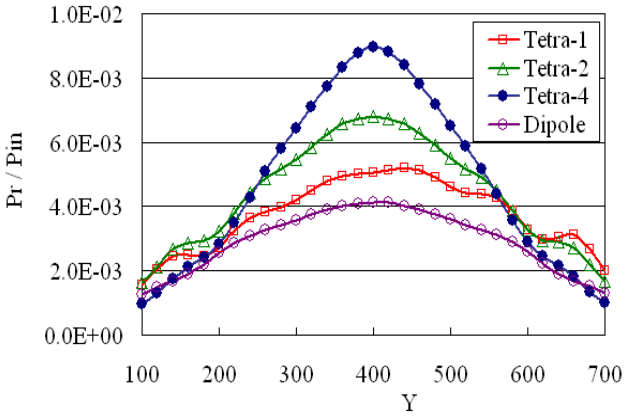

Figure 3. *Electromagnetic field distributions at Z=360. The vertical axis is the radiation intensity P_r/P_{in}, and the horizontal axis is the Y coordinate.*

Figure 3 is the result at frequency f_0 for the electromagnetic field, which is seen to strengthen at Y = 400, the center of the observation line. The frequency, f_0, of Tetra-1, 2, and 4 was 2.30, 2.25, and 2.25 GHz, respectively. A dipole antenna of 60 mm in length was also measured for comparison. The dipole was placed at the same position as the center of Tetra-4 as shown in Figure 2. The frequency f_0 of the dipole antenna was 2.20 GHz.

3.3. Various Characteristics

The simulated results for the relative frequency bandwidth (3dB), input impedance, radiation intensity P_r/P_{in}, antenna gain G, and the 3 dB range of beam width of Tetra-4 are given in Table 1 of Section 4 in comparison to those of a dipole. The real part of the input impedance of the dipole and Tetra-4 were 68 Ω and 492 Ω, respectively. Since the results were calculated using only the upper half, the actual input impedance is twice the value shown in the table. Moreover, the beam width is shown as a ratio to the distance, 329, between the antenna and the observation point. A real part of the input impedance of Tetra-1, Tetra-2, and Tetra-4 are 152 Ω, 318 Ω , and 592 Ω , respectively. The input impedance of Tetra-4 is very high with 592 Ω .

4. Experimental Results

In this section, we verify the operation of the Tetra-4 antenna through experimental measurements. Tetra-4 was installed in a balun with an impedance of 100 Ω. The power transmission was measured between broad band antennas placed 453 mm from our antenna. The gain of the antenna was 2.0 dBi. The measurement results are summarized in Table 1. The relative frequency bandwidth (3 dB) was 24%, and the real part of the input impedance was 360 Ω. The impedance is twice the value shown in the table since the balun converted an unbalanced 50 Ω line into a 100 Ω balanced line. The input impedance of Tetra-4 is considerably high with 360 Ω. Since we connected a 360 Ω load with a 100 Ω line, the return loss was 1.7 dB. The measured input impedance and the gain are values close to the calculation results shown in Table 1. The gain of the experimental result is 1 dB or more smaller. The difference corresponds to the return loss.

The dipole with a reflector was measured as well as the Tetra-4 antenna, and it can be seen from Table 1 that the gain was 5.3 dB. The input and gain of the measured antenna were a close match to those of the simulations given in Table 1.

Table 1. *A comparison of the calculated and experimental results. The upper part shows the calculated values while the lower part shows the experimental values.*

		dipole	Tetra-4
Computations	Relative bandwidth [%]	36	53
	Input impedance [Ω]	34+j7	246-j26
	Pr / Pin [dB]	-23.8	-20.5
	Gain G [dBi]	5.8	9.4
	3dB range (Y range / 329)	1.42	0.96
Experiments	Relative bandwidth [%]	37	24
	Input impedance [Ω]	37+j8	180+j87
	Gain G [dBi]	5.3	8.0
	HPBW [degrees]	87	38

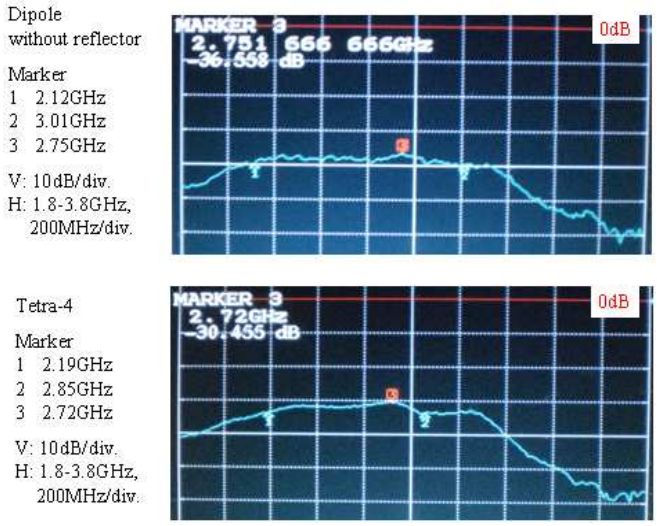

Figure 4. *Frequency characteristics of $|S_{21}|$. (a) Upper: A dipole without a reflector. (b) Lower: Tetra-4 antenna.*

Figure 4 shows a comparison of the power transmission characteristics of Tetra-4 and the half wavelength dipole antenna. Figure 4(b) shows the frequency characteristics of $|S_{21}|$ of Tetra-4. Here, S_{21} is a parameter of the scattering matrix. The frequency band (3 dB) was 2.19 - 2.85 GHz, and the flat level of $|S_{21}|$ was -30.5 dB. The half wavelength dipole antenna (without a reflector) was also measured, and had a gain of 2.0 dBi. The S_{21} characteristic is as shown in Figure 4(a). The frequency bandwidth (3 dB) was 2.12 - 3.01 GHz, and $|S_{21}|$ was -36.6 dB even when we read the largest point. Therefore, there was a 8 dB gain in Tetra-4, and this is confirmed by both the simulation and experimental data given in Table 1. As mentioned above, the experimental and simulated results are virtually identical.

Furthermore, Figure 5 shows the radiation patterns in the YZ plane (H-plane). Because a passive tag requires a strong

electromagnetic field, only a strong range of the radiation is shown. The sidelobe is -25dB or less. The half-power beam width (HPBW) was 38 degrees for the Tetra-4 antenna, whereas it was 87 degrees for the dipole antenna. The HPBW of Tetra-4 was 44% that of the dipole. For XZ plane (E-plane), the HPBW of Tetra-4 was 60 degrees.

When the direction in a horizontal plane is detected by arranging tag for a linearly polarized wave, the radiation pattern in a horizontal plane is important. The antenna with narrow beam width is necessary in a horizontal plane. Tetra-4 can be used for this purpose.

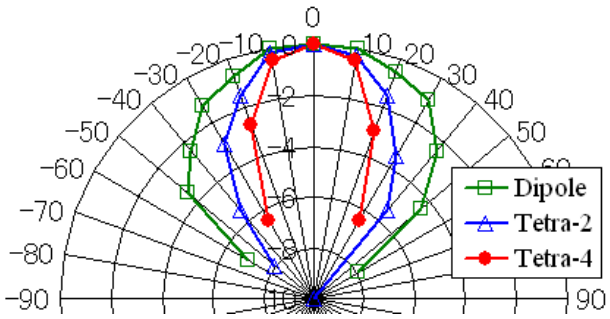

Figure 5. *Experimental radiation patterns in the YZ plane. A comparison of a dipole with a reflector, Tetra-2, and Tetra-4.*

5. Yagi-Uda Antenna

In this section, the Yagi-Uda antenna comprised of Tetra-1 elements is studied. Figure 6 shows the antenna structure. It consists of two Tetra-1 elements and a reflector. The antenna size is a=31mm, b=62mm, c=104mm, and d=128mm. The size of Tetra-1 far from the reflector is 10% smaller. This antenna is driven in balanced 50 Ω system. Figure 7 shows the experimental radiation patterns. Because a passive tag requires a strong electromagnetic field, only a strong range of the radiation is shown. The sidelobe is -30dB or less. The gain is 11dBi, with HPBW in the H-plane of 40 degrees and in the E-plane of 36 degrees. This antenna has the frequency bandwidth of 10% in frequency 2.54GHz. This antenna can be used to detect a vertical position in addition to the horizontal position.

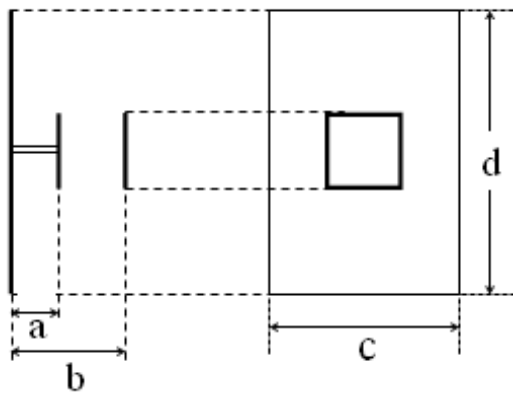

Figure 6. *Configuration of Yagi-Uda antenna conformed with two Tetra-1 elements.*

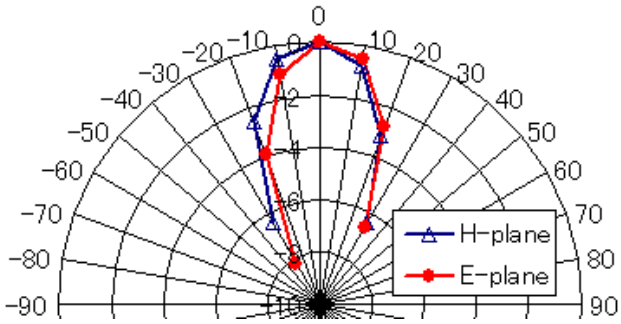

Figure 7. *Experimental radiation patterns of Yagi-Uda antenna using two Tetra-1 elements.*

6. Conclusions

In the field of location estimation using RFID technology, the antenna is a very important component. In this paper, a simple and small structural antenna was studied. Our design culminates in two antennas comprised of tetragon elements formed with wires.

One is an antenna, Tetra-4, which has a lateral arrangement of four tetragons made from conducting wire. Because the input impedance is considerably high, Tetra-4 is suitable for use in the high impedance system. Real part of the input impedance was 492 Ω in the simulation, and 360 Ω in the experiments. Antenna gain by the simulation is 9dBi. When driving in 100 Ω balanced system, the gain by the experiments was 8dBi. The experimental HPBW in the H-plane was 38 degrees, and was 0.44 times that of a dipole with a reflector.

Another one is Yagi-Uda antenna comprised of two tetragon elements. When driving in 50 Ω balanced system, the gain by experiments was 11dBi. The experimental HPBW was 40 degrees in the H-plane and was 36 degrees in the E-plane.

Acknowledgements

This research was partially supported by Grant-in-Aid for JSPS Fellows (No. 26･4643).

References

[1] Finkenzeller, G. K., RFID Handbook., Radio-frequency identification fundamentals and applications, John Wiley & Son, Chichester, 1999.

[2] Hähnel D., Burgard W., Fox D., Fishkin K., and Philipose M., “Mapping and localization with RFID technology,” Proc. 2004 IEEE International Conference on Robotics and Automation, vol. 1, pp. 1015-1020, New Orleans, USA, Apr. 2004.

[3] Manzoor F., Huang Y., and Menzel K., “Passive RFID-based indoor positioning system, an algorithm approach,” Proc. IEEE International Conference on RFID-Technology and Applications, Guangzhou, China, Jun. 2010.

[4] DiGiampaolo E., and Martinelli F., “A passive UHF-RFID system for the localization of an indoor autonomous vehicle,” IEEE Transactions on Industrial Electronics, vol. 59, no. 10, pp. 3961-3970, Oct. 2012.

[5] Wada T., Hori T., Fujimoto M., Mutsuura K., and Okada, H. "An adaptive multi-range-sensing method for 3D localization of passive RFID tags," IEICE Transactions on Fundamentals of Electronics, Communications and Computer Sciences, vol. E95-A, no. 6, pp. 1074-1083, Jun. 2012.

[6] Fujimoto M., Wada T., Inada A., Nakamori E., Oda Y., Mutsuura K., and Okada H., "Localization of passive RFID tags by using broad-type multi-sensing-range (B-MSR) method," IEICE Transactions on Fundamentals of Electronics, Communications and Computer Sciences, vol. E95-A, No. 7, pp. 1164-1174, Jul. 2012.

[7] Fujimoto M., Wada T., Inada A., Mutsuura K., and Okada H., "Swift communication range recognition method for quick and accurate position estimation of passive RFID tags," IEICE Transactions on Fundamentals of Electronics, Communications and Computer Sciences, vol. E95-A, no. 9, pp. 1596-1605, Sep. 2012.

[8] Kulyukin V., Gharpure C., Nicholson J., and Pavithran S., "RFID in robot-assisted indoor navigation for the visually impaired," Proc. 2004 IEEE/RSJ International Conference on Intelligent Robots and System, vol. 2, pp. 1979-1984, Sendai, Japan, Oct. 2004.

[9] Gueaieb W., and Miah S., "An intelligent mobile robot navigation technique using RFID technology," IEEE Trans. Instrum. Meas., vol. 57, no. 9, pp. 1908-1917, Sep. 2008

[10] Zou J., and Wang L., "Research of navigation and positioning at local area based on RFID," Proc. 2010 International Conference on Computer Application and System Modeling, vol. 11, pp. 5-8, Taiyuan, China, Oct. 2010.

[11] Fujimoto M., Nakamori E., Tsukuda D., Wada T., Mutsuura K., Okada H., and Iida Y., "A new indoor robot navigation system using RFID technology," Proc. 4th International Conference on Indoor Positioning and Indoor Navigation (IPIN 2013), pp. 637-638, Montbéliard, France, Oct. 2013.

[12] Park S., and Lee H., "Self-recognition of vehicle position using UHF passive RFID tags," IEEE Transactions on Industrial Electronics, vol. 60, No. 1, pp. 226-234, Jan. 2013.

[13] Ahmad M. Y., and Mohan A. S., "Novel bridge-loop reader for positioning with HF RFID under sparse tag grid," IEEE Transactions on Industrial Electronics, vol. 61, No. 1, pp. 555-566, Jan. 2014.

[14] Nagao R., Fujimoto M., Tsukuda D., Nakanishi T., Wada T., Mutsuura K., and Okada H., "Routing and moving control method using passive RFID for robot navigation system," Proc. 8th Annual IEEE International Conference on RFID (IEEE RFID 2014), pp.68-69, Orlando, USA, Apr. 2014.

[15] Wang J., Sang L., Wang Z., Xu R., and Yan B., "A broadband quasi-yagi array of rectangular loops on LTCC," Int. J. RF Microw Comput－Aided Eng, vol.24, no.2, pp.196-203, Mar. 2014.

[16] Kim S. -G., Zepeda P., and Chang K., "Piezoelectric transducer controlled multiple beam phased array using microstrip rotman lens," IEEE Microwave Wireless Compon. Lett., vol.15, no.4, pp.247-249, Apr. 2005.

[17] Li M., and Luk K.-M., "A low-profile unidirectional printed antenna for millimeter-wave applications," IEEE Trans Antennas Propag., no.3, pp.1232-1237, Mar. 2014.

[18] Tsutsumi Y., Ito T., Hashimoto K., Obayashi S., Shoki H., and Kasami H., "Bonding wire loop antenna in standard ball grid array package for 60-GHz short-range wireless communication," IEEE Trans Antennas Propag, vol.61, no.4, Pt.1, pp.1557-1563, Apr. 2013.

[19] Haider N., Caratelli D., and Yarovoya G., "Circuital characteristics and radiation properties of an UWB electric-magnetic planar antenna for Ku-band applications," Radio Sci., vol.48, no.1, pp.13-2, Jan. 2013.

[20] Yuan X., Wong K. T., Xu Z., and Agrawal K., "Various compositions to form a triad of collocated dipoles/loops, for direction finding and polarization estimation," IEEE Sens J., vol.12, no.5－6, pp.1763-1771, May 2012.

[21] Yasin M. N. M., and Khamas S. K., "Measurements and analysis of a probe-fed circularly polarized loop antenna printed on a layered dielectric sphere," IEEE Trans Antennas Propag., vol.60, no.4, pp.2096-2100, Apr. 2012.

[22] Pal A., Mehta A., Mirshekar‐Syahkal D., Deo P., and Nakano H., "Dual-band low-profile capacitively coupled beam-steerable square-loop antenna," IEEE Trans Antennas Propag., vol.62, no.3, pp.1204-1211, Mar. 2014.

[23] Gupta S., and Mumcu G., "Dual-band miniature coupled double loop GPS antenna loaded with lumped capacitors and inductive pins," IEEE Trans Antennas Propag., vol.61, no.6, pp.2904-2910, Jun. 2013.